Preparation-dependent Co/Si(100) (2×1) interface growth: Spontaneous silicide formation versus interstitial-site mechanism

H. L. Meyerheim*
Sietec GmbH, Röntgenmessplatz bei der Berliner Elektronenspeicherring-Gesellschaft für Synchrotronstrahlung (BESSY), Lentzeallee 100, D-1000 Berlin 33, Germany
and Institut für Experimentalphysik der Freien Universität Berlin, Arnimallee 14, D-1000 Berlin 33, Germany

U. Döbler and A. Puschmann
Sietec GmbH, Röntgenmessplatz bei der Berliner Elektronenspeicherring-Gesellschaft für Synchrotronstrahlung (BESSY), Lentzeallee 100, D-1000 Berlin 33, Germany

(Received 12 February 1990; revised manuscript received 7 March 1991)

Extended x-ray-absorption fine-structure measurements, low-energy electron diffraction, and Auger-electron spectroscopy have been applied to study preparation-dependent room-temperature Co/Si(100) interface formation. Evaporation of Co onto chemically etched and annealed Si(100) (2×1) leads up to about 0.5 monolayer coverage for adsorption of Co in the fourfold-hollow sites of the locally unreconstructed Si(100) surface. At higher coverages Co atoms occupy interstitial (adamanthane) and substitutional sites of the Si lattice. Annealing at $T=550$–$650\,^{\circ}C$ for 5 min induces the diffusion of Co into the Si lattice, where Co atoms reside in adamanthane sites only. After evaporation of Co onto sputter-annealed Si(100) (2×1), only the formation of a locally ordered $CoSi_2$-like phase could be observed in the measured coverage regime between 0.8 and 14 monolayers.

I. INTRODUCTION

The room-temperature (RT) nucleation of Co on Si(100) has not, to our knowledge, been investigated previously, and only a few experiments concerned with the chemically very similar Ni/Si(100) system have been reported. Helium-channeling experiments[1] and ultraviolet-photoelectron-spectroscopy data[2] compared with band-structure calculations[3] support the picture of Ni atoms incorporated into the interstitial adamanthane site in the center of the Si unit cell,[4] where the metal atom is surrounded by four nearest-neighbor Si atoms and by six second-nearest Si atoms located at the corners of a tetrahedron and octahedron, respectively. In contrast, total-energy calculations[5] do not agree with the adamanthane site and favor the fluoritelike sixfold-coordinated interstitial site as observed for the Ni/Si(111) interface.[6]

In order to analyze the Co/Si(100) interface structures, which form by evaporation of Co onto differently prepared Si(100) surfaces at RT and by annealing the deposited interfaces, we applied the surface-extended x-ray-absorption fine-structure (SEXAFS), the low-energy electron-diffraction (LEED), and the Auger-electron-spectroscopy (AES) techniques.

In the following, we consider the initial adsorption site of Co evaporated onto Si(100) (2×1) which was prepared by etching in hydrofluoric acid (HF) and annealing [$Si(100)_{HF}$]. In Sec. III the initial adsorption behavior of Co on sputter-annealed Si(100) (2×1) [$Si(100)_{Ar}$] is investigated and compared with the initial $Co/Si(100)_{HF}$ interface formation. The structural evolution of the $Co/Si(100)_{HF}$ interface at higher Co coverages and after annealing is presented in Sec. IV. In Sec. V the results are discussed on the basis of the existing literature and summarized in Sec. VI.

II. INITIAL ROOM-TEMPERATURE ADSORPTION OF Co ON $Si(100)_{HF}$

The Si(100) wafers were prepared by wet chemical etching in 20 vol % HF followed by annealing at 850 °C after transfer into the UHV chamber. A sharp (2×1) LEED pattern could be observed and neither oxygen nor carbon contaminants were determined by Auger-electron spectroscopy (AES).

The metal evaporation onto Si(100) was performed by resistive heating of a Co wire. During evaporation the pressure was below 2×10^{-10} mbar (base pressure of 5×10^{-11} mbar). Within an error of about 10%, the number of adsorbed Co atoms was determined subsequently by Rutherford-backscattering spectroscopy for several samples, which in turn were used for the calibration of other samples by comparing Co/Si AES intensity ratios or absorption-edge jumps J_R measured in the total-electron-yield (TEY) mode.[7] This procedure leads to an accuracy of about 15–25 %.

After the evaporation of 0.4 monolayer (ML) of Co onto $Si(100)_{HF}$, the (2×1) LEED pattern, which is characteristic for the clean Si(100) surface, was still observable, although the brightness of the spots was reduced. The local structural environment of the adsorbed Co atoms was determined by SEXAFS measurements. X-ray polarization-angle-dependent SEXAFS spectra were recorded above the Co $L_{II,III}$ edge in the TEY mode

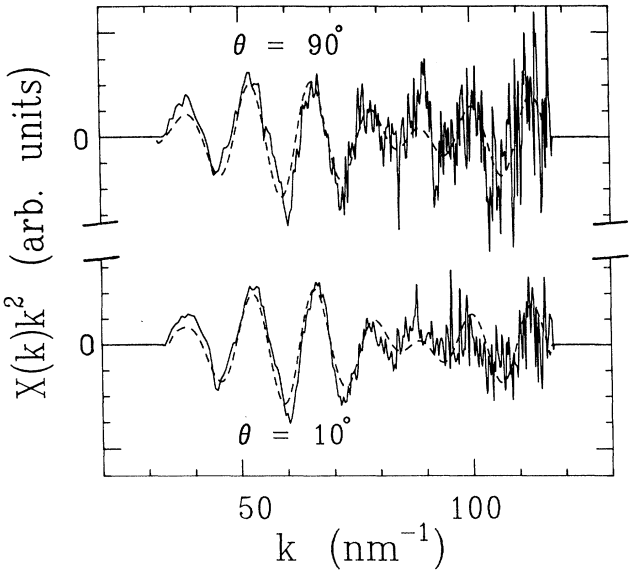

FIG. 1. Polarization-dependent SEXAFS spectra for 0.4-ML Co adsorbed on etch-annealed Si(100) at room temperature shown as solid lines. Simulations are superimposed on the experimental spectra as dashed lines.

using the SX 700 monochromator at the Berliner Elektronenspeicherring Gesellschaft für Synchrotronstrahlung mbH (BESSY). The data analysis was performed using the conventional Fourier transform (FT) technique[8,9] and by comparison with simulations.

Figure 1 shows as solid lines polarization-dependent SEXAFS spectra measured at normal ($\theta=90°$) and grazing ($\theta=10°$) x-ray incidence after evaporation of 0.4 ML Co. The corresponding FT spectra are shown in Fig. 2.

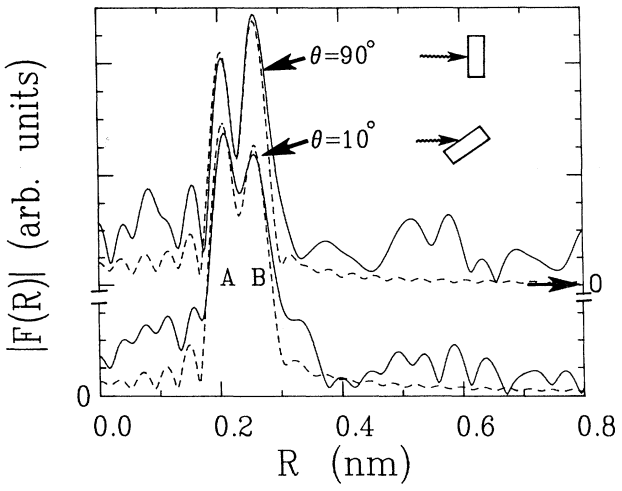

FIG. 2. Fourier transforms (FT's) of the SEXAFS spectra shown in Fig. 1. Corresponding simulations are shown as dashed lines. The peaks A and B correspond to Si shells located at distances of 0.230(2) and 0.280(5) nm, respectively. The distances and the polarization dependence of peak B indicate that Co is adsorbed at the Si(100) surface as shown in Fig. 3.

They are characterized by peaks labeled A and B, both originating from Si atoms.

The SEXAFS spectra were simulated using the single-scattering plane-wave formalism and are superimposed on the experimental spectra in Figs. 1 and 2 as dashed lines. It was proven that multiple-scattering effects are unimportant if only shells A and B are considered. Some deviations between experimental and simulated SEXAFS spectra in Figs. 1 and 2 are due to the neglect of low- and high-frequency contributions which arise from errors in the background subtraction procedure and from noise, respectively. Good agreement can only be obtained for Co adsorbed nearly in plane ($d_\perp=0$) of the unreconstructed Si(100) surface as shown in Fig. 3. Shell A corresponds to two Si atoms in the second layer shown as open dashed circles. Shell B consists of five Si atoms, four in the first, one in the third layer, shown as hatched circles. Si atoms B form a "fourfold hollow"; therefore, we assign the adsorption site as a fourfold hollow site, although the nearest-neighbor Si atoms (A) form a bridge site.

The neighbor distances for the 0.4-ML coverage sample were determined to be $R_A=0.230(3)$ nm and $R_B=0.280(5)$ nm using the experimentally derived Co-Si scattering phase shift $\Phi_{(\mathrm{Co-Si})}=4.54-0.044k$ (nm^{-1}) obtained from a $CoSi_2$ reference sample.

The effective coordination numbers N_A^* and N_B^* used for the simulations assuming surface adsorption are listed in Table I. N_A^* is determined to be 2 and independent of θ; for N_B^* we calculated 5.3 ($\theta=90°$) and 4.4 ($\theta=10°$).

The short-range order structure determination shows that upon Co adsorption the (2×1) reconstruction of the Si(100) surface is lifted. Assuming a rigid Si structure, lattice distances of $R_A=0.235$ nm and $R_B=0.272$ nm are calculated for surface ($d_\perp=0$) adsorption. The comparison with the experimental data [$R_A=0.230(3)$ nm and $R_B=0.280(5)$ nm] indicates a distortion of the Si structure. It is not possible to match the experimentally derived distances R_A and R_B simultaneously by variation of $d_\perp$ only.

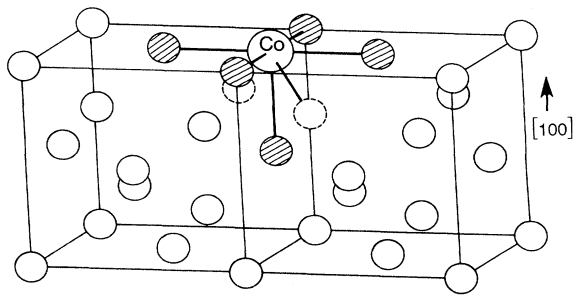

FIG. 3. Surface adsorption site as determined for Co evaporated onto etch-annealed Si(100) at about 0.4 ML. Two Si unit cells are shown. Shell A corresponds to two Si atoms shown as open dashed circles, shell B corresponds to five Si atoms shown as hatched circles.

TABLE I. Calculated effective coordination numbers for Co adsorbed on the Si(100) surface and incorporated into the interstitial adamanthane site for normal and grazing incidence. The corresponding calculated amplitude ratios between the shells A and B are compared with the experimental data measured after adsorption of 0.4-ML Co onto etch-annealed Si(100).

	N_A^*		N_B^*	
	90°	10°	90°	10°
Surface Site $N_i^*(90^0)/N_i^*(10^0)$	2.0	2.0	5.3	4.4
	1.00		1.20	
Interstitial Site $N_i^*(90^0)/N_i^*(10^0)$	4.0	4.0	6.0	6.0
	1.00		1.00	
Experiment $N_i^*(90^0)/N_i^*(10^0)$	1.02 (10)		1.27 (12)	

The incorporation of Co into the interstitial adamanthane site in the center of the Si unit cell (Fig. 4) can be ruled out. In this position the Co atom is surrounded by four nearest Si atoms (shell A, shown as open dashed circles) and by six second-nearest neighbors (shell B, shown as hatched circles), located at the corners of a tetrahedron and octahedron, respectively. Although the distances in this position are expected to be very similar to those for the surface site, the distinction can be done on the basis of the effective coordination numbers (Table I).

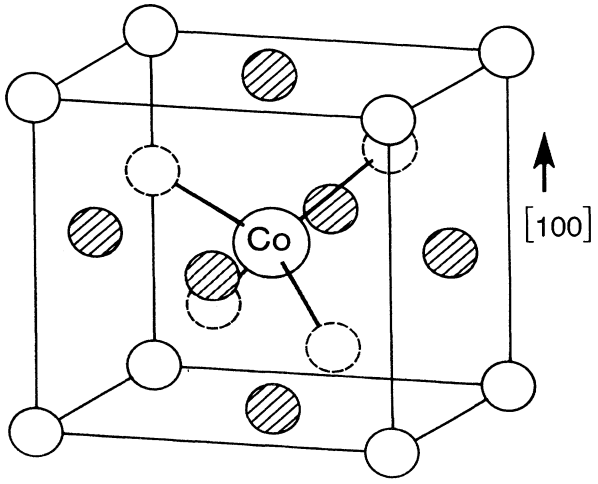

FIG. 4. Interstitial (adamanthane) site of Co in the center of the Si unit cell. The Co atom is neighbored by four nearest-neighbor Si atoms located at the corners of a tetrahedron (shell A, open dashed circles), and by six second-nearest Si neighbors located at the corners of an octahedron (shell B, hatched circles).

There is only a 10–25 % difference for N_B^* between surface and interstitial site adsorption but a 100% difference for N_A^*, which is far out of the experimental uncertainty. The incorporation of Co into the interstitial site is discussed in Sec. IV in more detail. At 0.4-ML coverage a (2×1) LEED pattern is still observable, although the brightness of the spots is reduced as compared to the clean Si(100) surface. Therefore, we propose that only adsorption sites in every second [110] row of the Si(100) surface are occupied by Co atoms creating a new (2×1) superstructure.

Other adsorption sites like bridge, atop, or different interstitial sites[6] as well as Si substitution can already be ruled out by the experimental distance data. This is especially true for the formation of stoichiometric Co silicide structures by interface reactions as was confirmed by comparison of experimental and simulated spectra. Moreover, silicide formation would rapidly disrupt the (2×1) LEED pattern.

III. PREPARATION DEPENDENCE OF THE INITIAL Co/Si(100) ADSORPTION

In a second experiment, Co was evaporated onto Si(100) (2×1), which was cleaned by repetitive cycles of Ar^+ ion sputtering (1.0–1.5 kV) followed by annealing at 850 °C. In the upper part of Fig. 5, FT spectra obtained at normal incidence after evaporation of about 0.8-ML Co onto $Si(100)_{Ar}$ (dashed line) and of polycrystalline $CoSi_2$ used as a reference sample (solid line) are compared. In order to elucidate the differences in the adsorption behavior between the two surface preparations we have added in the lower part of Fig. 5 an FT spectrum obtained for a 0.8-ML $Co/Si(100)_{HF}$ sample at normal incidence showing peaks A and B discussed in the previous section.

In the $CoSi_2$ reference and the 0.8-ML $Co/Si(100)_{Ar}$ spectra the peaks A and C are correlated to Si and Co backscatterers, respectively. Using the experimentally derived scattering phase shift the Co—Si bond length of the 0.8-ML $Co/Si(100)_{Ar}$ spectrum is determined to $R_A = 0.237(4)$ nm as compared to $R_A = 0.232$ nm in $CoSi_2$. Using the "log ratio" method[10] we determined a coordinate number $N_A^* = 8.9$ around the Co atoms in the interface structure. Within an error bar of about 10–20 % for the EXAFS amplitude analysis, this is in agreement with $N_A^* = 8$ in $CoSi_2$. The 0.8-ML $Co/Si(100)_{Ar}$ spectrum is representative for all measured coverages up to about 14 ML.

By direct comparison with the 0.8-ML $Co/Si(100)_{HF}$ spectrum it is evident that the adsorption behavior depends on the surface preparation. Sputter annealing leads to the formation of a locally ordered $CoSi_2$-like structure, whereas after etch-annealing the evaporated Co atoms occupy well-defined adsorption sites of the intact Si structure as discussed in the previous section.

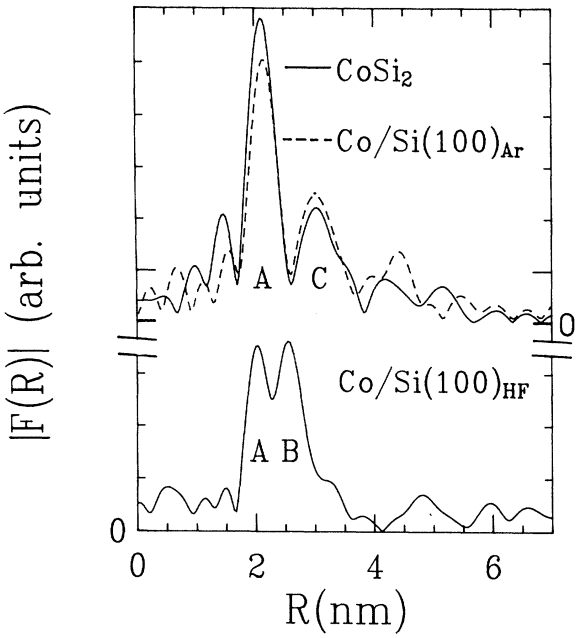

FIG. 5. Comparison of FT spectra obtained after RT evaporation of about 0.8-ML Co onto etch annealed Si(100) (lower part) and on sputter-annealed Si(100) (upper part). The adsorption of Co on $Si(100)_{Ar}$ leads to the formation of a locally ordered $CoSi_2$-like structure. This is evident by comparison of the 0.8-ML spectrum (dashed line) with the $CoSi_2$ reference spectrum (solid line). Peaks *A* and *C* correspond to Si and Co backscatterers, respectively. The comparison with the $Si(100)_{HF}$ spectrum directly indicates the preparation dependence of the Co/Si(100) interface formation.

The preparation dependence is observed in AES and LEED measurements as well. In Fig. 6 the 92-eV Si (*LVV*) peak-to-peak Auger intensity is shown versus Co coverage. For evaporation of Co onto $Si(100)_{Ar}$ only a slowly decreasing Si Auger intensity is observed indicating strong Co-Si intermixing. In contrast, adsorption of Co on $Si(100)_{HF}$ results in a much more complicated interface formation, which can be divided into four different regimes labeled I–IV. In order to exactly determine the limits of the regimes I and II we have performed several experiments using different evaporation rates. All experiments are summarized in Fig. 6. The rapidly decreasing signal intensity in regime I can be explained by the formation of a Co adlayer on the surface as discussed above. Assuming homogeneous metal overgrowth and a monolayer thickness of $d_{Co}=0.25$ nm, the signal attenuation is correlated to a mean free path of the Si (*LVV*) Auger electrons of $\lambda=0.5$ nm, which is in reasonable agreement with published data.[11] The surface adsorption stops at about 0.5-ML coverage. This is consistent with the proposed (2×1) adsorbate structure, since this structure model allows only 0.5-ML Co to adsorb at the surface. The structural evolution at higher coverages is discussed in the following section.

IV. STRUCTURAL EVOLUTION OF THE $Co/Si(100)_{HF}$ INTERFACE AT HIGHER COVERAGE AND AFTER ANNEALING

Figure 7 shows a sequence of FT spectra which were derived from normal incidence EXAFS data. They were measured after evaporation of Co onto $Si(100)_{HF}$ in the coverage regime between 0.8 and 13.6 ML. With increasing coverage the FT peak positions are hardly affected,

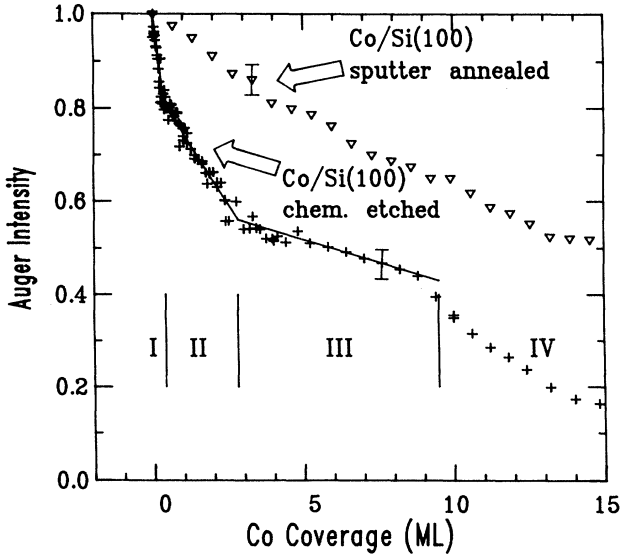

FIG. 6. Si (*LVV*) Auger intensity shown as a function of Co coverage for both preparation procedures. For Co evaporated onto sputter-annealed Si(100) a slowly decreasing Si Auger intensity is observed indicating strong Co-Si intermixing. For Co evaporated onto etch-annealed Si(100) four regimes I–IV can be distinguished.

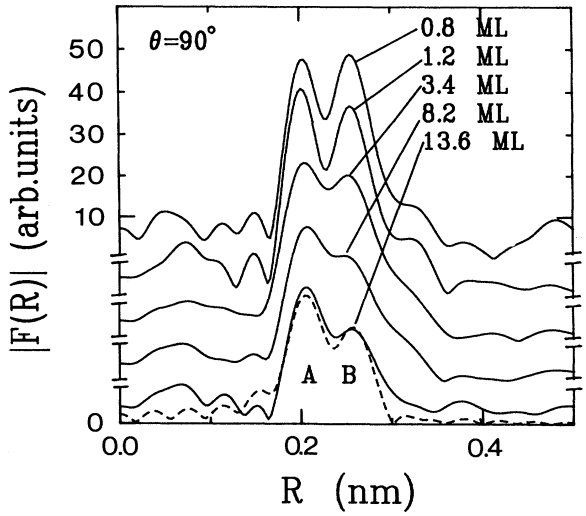

FIG. 7. FT spectra of normal incidence EXAFS data for Co coverages between 0.8 and 13.6 ML evaporated onto etch-annealed Si(100). The spectra are successively shifted by 10 units for clarity. With increasing coverage the amplitude ratio *A*/*B* increases while the absolute intensity of both peaks decreases. A simulation for the 13.6-ML spectrum is shown as a dashed line.

but we observe an increasing amplitude ratio A/B and a decreasing absolute amplitude for both peaks. These observations are due to incorporation of Co into the interstitial site (Fig. 4) and due to Co-Si substitution, respectively.

Upon incorporation of Co into the interstitial site the effective nearest-neighbor coordination rises by 100% from $N_A^*=2$ at the surface to $N_A^*=4$ in the interstitial site, but N_B^* increases only by about 10% (Table I). This leads to an increasing intensity of peak A relative to peak B.

The reduction of the absolute amplitude can be estimated by looking at peak B because N_B^* does not depend strongly on the adsorption sites discussed. The 50% amplitude reduction observed for the 13.6-ML sample compared to the 0.8-ML sample can be explained by the substitution of Si host lattice atoms by Co. This can be understood from the backscattering phase-shift difference $\Delta\Phi=\Phi_{(\text{Co-Si})}-\Phi_{(\text{Co-Co})}$ between Co-Si and Co-Co pairs which is nearly π throughout the whole SEXAFS data range.[12] This antiphase contribution leads to the reduction of the EXAFS amplitude for each substituted Si atom due to negative interference. The amplitude reduction is significant at coverages above 2–3 ML. The 13.6-ML case can be simulated by assuming a statistical substitution of about 25% host lattice Si atoms (see dashed line in Fig. 7).

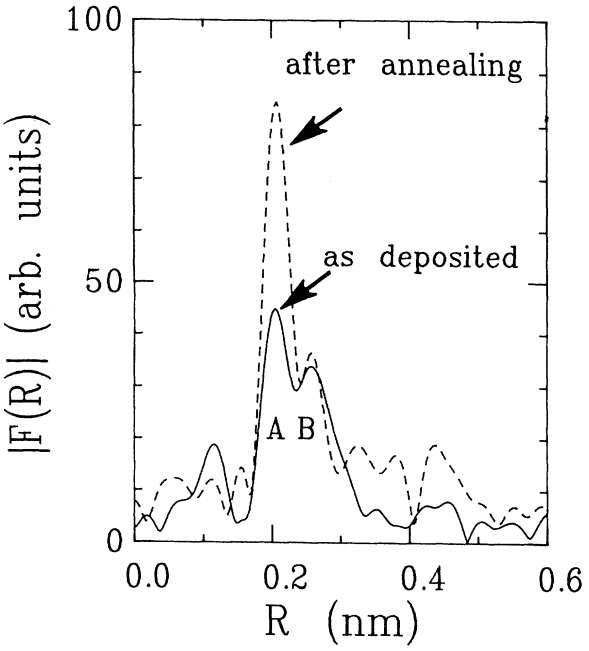

FIG. 9. FT spectrum of 1.2-ML Co on etch-annealed Si(100) before (solid line) and after annealing (dashed line). The 100% increase of peak A amplitude indicates the incorporation of Co into interstitial adamanthane sites.

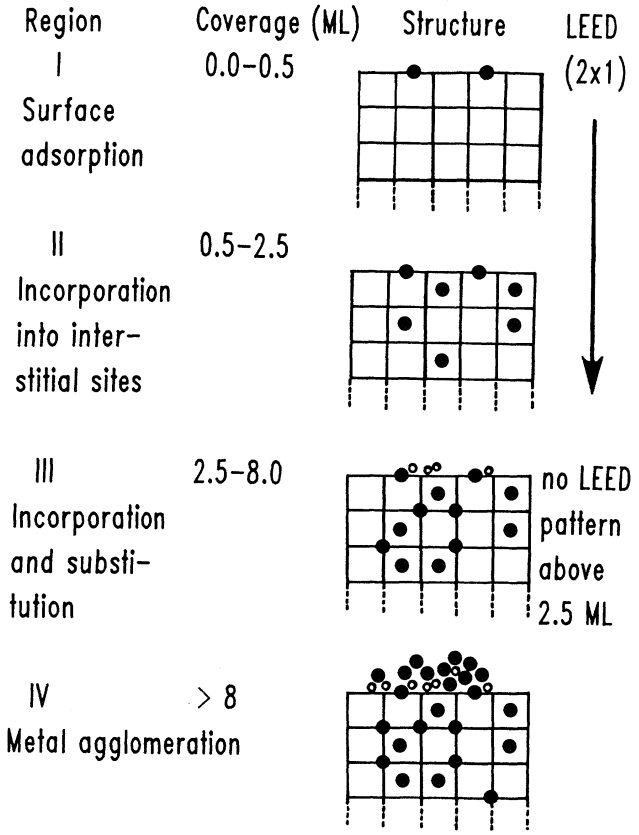

FIG. 8. Summary of the RT-interface formation sequence for etch-annealed Si(100) based on the EXAFS, AES, and LEED data. Filled circles represent Co atoms, open circles represent Si atoms set free by substitution processes. Si host lattice atoms are located at the line intersections. Four regimes of interface formation labeled I–IV can be distinguished.

Both Co incorporation and Co-Si substitution also explain the AES data (Fig. 6). The surface-sensitive Si (LVV) Auger signal is less attenuated by incorporated Co atoms in regime II than by surface-adsorbed Co atoms in regime I. Moreover, at the beginning of regime III, the AES signal decreases even more slowly and the LEED pattern vanishes. This is compatible with the idea that substituted Si atoms diffuse to the sample surface disrupting the long-range order. The structural evolution of the RT $\text{Co/Si(100)}_{\text{HF}}$ interface formation is schematically summarized in Fig. 8. Finally, at about 19-ML coverage a locally ordered metallic overlayer starts to grow.

After annealing the RT deposited samples in the temperature regime between 550 °C and 650° C all Co atoms reside in the interstitial sites. Within the measured regime between 1.2 and 19 ML this does not depend on the initial coverage.

Figure 9 shows two FT spectra obtained from a 1.2-ML sample before and after annealing. The doubling of the absolute peak A amplitude is consistent with 100% increase of N_A^* on going from the surface adsorption site to the intersitial site, whereas N_B^* is constant within the error bar. Higher distance shells which are compatible with the interstitial site are observable as well and were analyzed taking multiple-scattering effects into account.[13] Further evidence for the indiffusion of the Co atoms into

the substrate lattice comes from AES and LEED data as well. At low initial coverages (1.2 ML) annealing leads to the complete disappearance of the 54-eV Co (*MNN*) Auger signal and to the recovery of the bright (2×1) LEED pattern characteristic for the clean Si(100) surface. At high coverages the Co (*MNN*)/Si (*LVV*) AES intensity ratio is reduced by about 2 orders of magnitude.

V. DISCUSSION

The RT Co/Si(100) interface formation was found to depend on the surface preparation procedure. A higher density of structural defects created at the Si(100) surface by sputter annealing than by etch-annealing is assumed to be responsible for the different interface reactivities. The strong Co-Si reaction might be the consequence of sputter-induced defects like unsaturated or distorted bonds, which could not be removed by annealing. These act as nucleation centers for the spontaneous silicide reaction, where a locally ordered $CoSi_2$-like structure is formed. The first phase rule[14] predicting the initial formation of Co_2Si is not violated, because after surface preparation the system is not in thermodynamical equilibrium. On the other hand, a complicated Co/Si(100) interface formation consisting of four different regimes is observed for etch-annealed surfaces. In the beginning, Co adsorbs at the Si(100) surface and no Co-Si substitution processes are energetically possible unless about 2 ML of Co are incorporated into the interstitial sites of the Si host lattice. This mechanism corresponds to Tu's interstitial reaction path.[15] The first phase rule is not violated as well, because the interstitial adamanthane structure does not correspond to a stable phase in the binary Co-Si phase diagram. We did not determine the formation of epitaxial $CoSi_2$ (CaF_2 structure), which probably requires higher Co coverages and/or different preparation conditions.[16,17]

Contradictions between previous experiments dealing with the RT adsorption of Ni on Si(100) (Refs. 1 and 2) and calculations[5] might be lifted by taking the metal-Si substitution into account, which could stabilize the interstitial site occupation in larger quantities ($\theta > 1-2$ ML). Hamann and Mattheiss[5] find "the proposed diffusion region of interstitial Ni several atomic layers thick highly unfavorable energetically." However, the substitution processes were not considered nor observed in the He channeling experiments, which were probably not sensitive enough to detect a low concentration of Ni atoms statistically distributed at host lattice sites.

The redistribution of surface-adsorbed and substituted Co atoms into interstitial sites requires higher temperatures and is consistent with the assumption that the pure incorporation of Co into the interstitial sites is energetically unfavorable.

VI. SUMMARY

In this paper we have presented a detailed structural analysis of the Co/Si(100) interface formation at room temperature using SEXAFS, AES, and LEED. It could be shown that the Si(100) surface-cleaning procedure has strong influence on the local structure formed after Co adsorption.

A spontaneous interface reaction is observed after Co adsorption onto sputter annealed Si(100), whereas a more complicated reaction sequence basically corresponding to Tu's interstitial mechanism follows for etch-annealed surfaces. In the latter case direct evidence could be given for the incorporation of Co into the interstitial adamanthane site, which has been the subject of some controversy in the past, probably due to the neglect of metal-Si substitution processes.

The deep indiffusion of Co atoms into the Si host lattice is induced by annealing the $Co/Si(100)_{HF}$ interface. All Co atoms reside in interstitial adamanthane sites independent of the initial coverage measured up to 19 ML.

ACKNOWLEDGMENTS

We would like to thank the Siemens AG Corp. Research and Development for supporting this study, K. Wittmaack (Gesellschaft für Strahlen und Umweltforschung, München Neuherberg) for performing the Rutherford backscattering experiments, and D. Arvanitis (Freie Universität Berlin) for helpful discussions.

*Present address: Institut für Kristallographie und Mineralogie der Universität München, Theresienstrasse 41, 8000 München 2, Germany.

[1]N. W. Cheung and J. W. Mayer, Phys. Rev. Lett. **46**, 671 (1981).

[2]Yu-Jeng Chang and J. L. Erskine, Phys. Rev. B **28**, 5766 (1983); **26**, 4766 (1982).

[3]O. Bisi, L. W. Chiao, and K. N. Tu, Phys. Rev. B **30**, 4664 (1984).

[4]F. A. Cotton and G. Wilkinson, *Advanced Inorganic Chemistry* (Wiley, New York, 1980), p. 59.

[5]D. R. Hamann and L. F. Mattheiss, Phys. Rev. Lett. **54**, 2517 (1985).

[6]F. Comin, J. E. Rowe, and P. H. Citrin, Phys. Rev. Lett. **51**, 2402 (1983).

[7]For details of the yield techniques we refer to J. Stöhr, in *Principles, Applications, Techniques of EXAFS, SEXAFS, and XANES,* edited by D. C. Koningsberger and R. Prins (Wiley Interscience, New York, 1988), Chap. 10.

[8]P. A. Lee, P. H. Citrin, P. Eisenberger, and B. M. Kincaid, Rev. Mod. Phys. **53**, 769 (1981).

[9]D. E. Sayers and B. A. Bunker, in *Principles, Applications, Techniques of EXAFS, SEXAFS, and XANES* (Ref. 7), Chap. 6.

[10]For details of the "log ratio" method see *Principles, Applications, Techniques of EXAFS, SEXAFS, and XANES* (Ref. 7), Chaps. 6 and 10.

[11]M. P. Seah and W. A. Dench, Surf. Inter. Anal. **1**, 2 (1979).

[12]The experimentally derived Co-Co phase obtained from a thick ($\Theta > 100$ ML) evaporated Co layer is $\Phi_{(Co\text{-}Co)} = 1.27-0.039k$ (nm^{-1}). Correspondingly $\Delta\Phi = 3.27-0.005k$ (nm^{-1}).

[13]H. L. Meyerheim, Thesis, Freie Universität Berlin, 1990.
[14]R. M. Walser and R. W. Bene', Appl. Phys. Lett. **28**, 624 (1976).
[15]K. N. Tu, Appl. Phys. Lett. **27**, 221 (1975).
[16]A. H. von Ommen, C. W. T. Bulle-Lieuwma, and C. Langereis, J. Appl. Phys. **64**, 2706 (1988).
[17]S. M. Yalisove, R. T. Tung, and D. Loretto, J. Vac. Sci. Technol. A **7**, 1472 (1989).